Electronic Supplementary Material (ESI) for Journal of Materials Chemistry B.

One pot synthesis of monodisperse water soluble iron oxide nanocrystals with high values of specific absorption rate

*Pablo Guardia†, Andreas Riedinger†, Simone Nitti†, Giammarino Pugliese†, Sergio Marras†, Alessandro Genovese†, Maria Elena Materia†, Christophe Lefevre% Liberato Manna†, Teresa Pellegrino†**

† Nanochemistry, Istituto Italiano di Tecnologia,Via Morego 30, I-16163 Genova (Italy)

% Institut de Physique et Chimie des Matériaux de Strasbourg UMR 7504 CNRS - Université de Strasbourg

RATE °C/min	**Fe mmol**	**Dec mmol**	**DBE ml**	**Squalane ml**	**Size nm**	**Deviation nm**
7	1	4	3	22	100	11
7	1	4	4	21	47	4.1
7	1	4	5	20	38	3.5
7	1	4	7	18	26	2.5
7	1	4	9	16	22	2.5
7	2	8	18	32	22	4.5(&)
7	1	4	18	7	18	1.9
7	1	4	18	7	21	3
7	1	4	20	5	18	2.1
7	1	4	23	2	14	1.9
7	1	5	15	10	17	1.5
7	1	6	15	10	14	1.3
2.5	1	4	15	10	28	2.2
1.6	1	4	15	10	31	3
7	1	4	15	10	14	1.5(*)
7	1	4	18	7	19	2(*)
7	1	4	15	10	24	2(*)

7	1	4	7.5	17.5	35	2(*)

Table S1. Summary of some synthesis parameters used for iron oxide nanocubes of different sizes. Note that for all synthesis a vacuum step (120 minutes at 65 °C and a p = 0. 1mmbar) was performed. (*) Particles used for the SAR analysis. (&) In this synthesis conditions by doubling the amount of precursors to obtain 70 mg in iron of nanocubes of 22 nm in size with respect to 30 mg of the other synthesis (see also Figure S5 for TEM characterization).

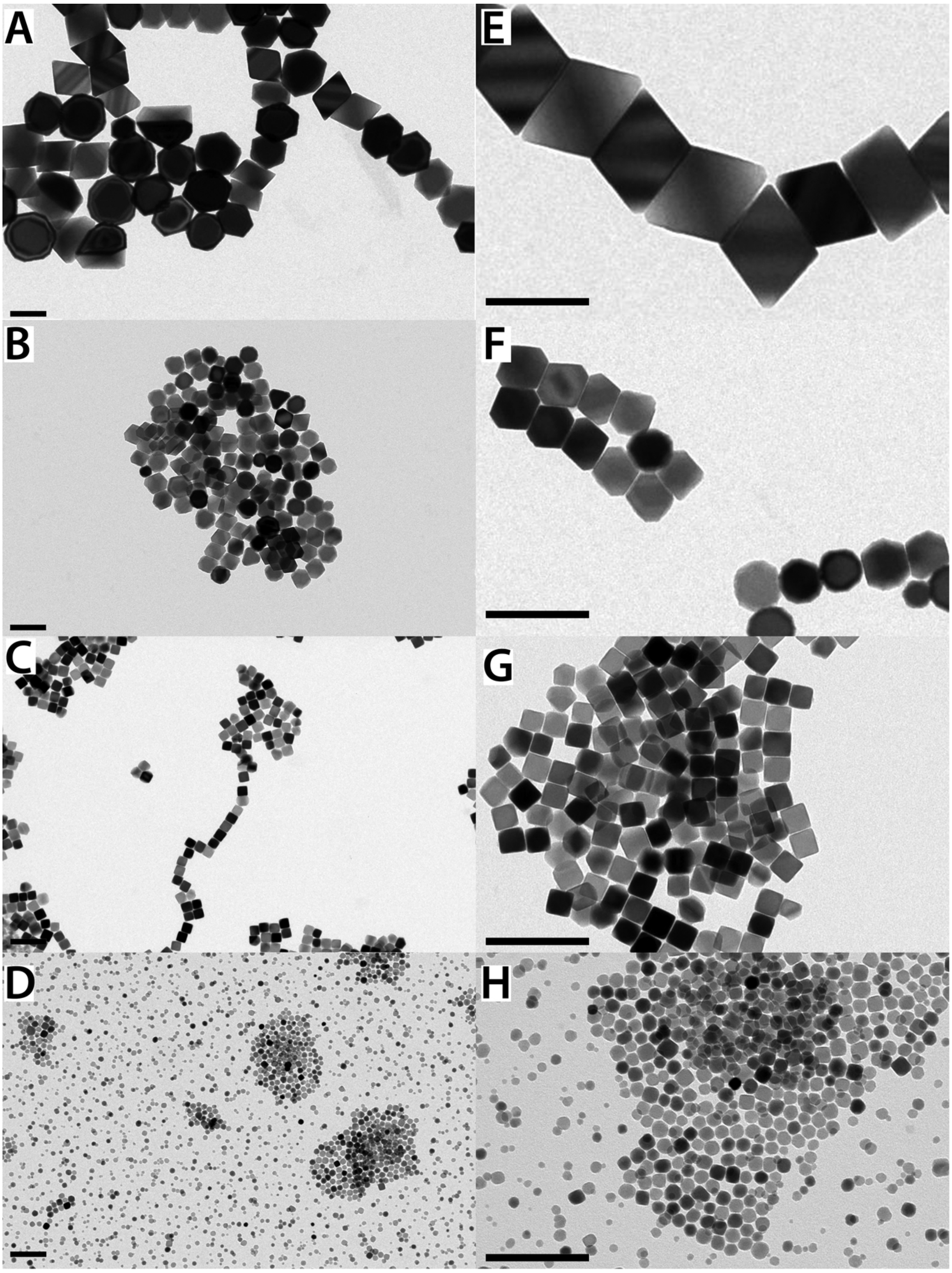

Figure S1. Representative transmission electron microscopy for iron oxide nanocubes produced using the conditions specified above. A) 100 ± 7 nm, B) 38± 4 nm, C) 26 ± 2 nm and D) 14 ± 2 nm by using A) 3 mL, B) 4 mL, C) 7 mL and D) 23 mL of DBE (the total solvent volume is fixed at 25 mL and the difference in volume is provided by squalane). Scale bars correspond to 100 nm. The mean size and the standard deviation for all the TEM figures were calculated by measuring at least 100 particles.

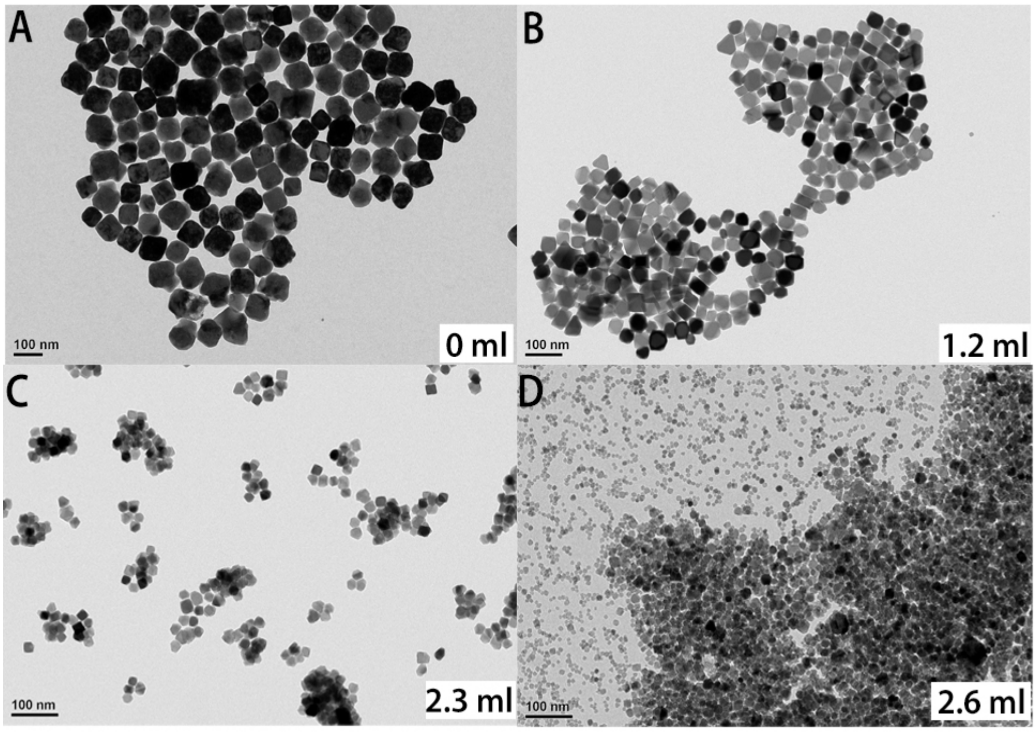

Figure S2. The effect of benzaldehyde on the synthesis of iron oxide nanocubes of A) 81 ± 15 nm, B) 40± 4 nm, C) 19 ± 3 nm and D) 16 ± 10 nm edge length synthesized using 1 mmol of iron acetylacetonate, 4 mmols of decanoic acid, a heating rate of 7 °C/minutes, 22 mL of squalane and A) 0 ml, B) 1.2 ml(12mmols), C) 2.3 ml (22.5 mmols) and D) 2.6 ml (25.5 mmols) of benzaldehyde.

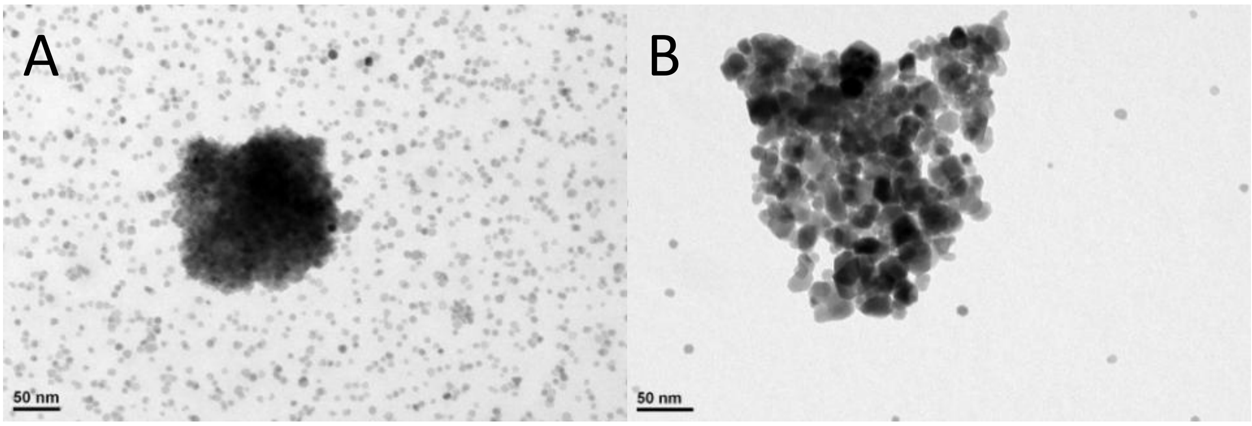

Figure S3. Effect of the benzyl alcohol on iron oxide nanocubes synthesis by using 1 mmol of iron acetylacetonate, 4 mmols of decanoic acid, 22 ml of squalane, and after introducing A) 1.2 mL (11.6 mmols), and B) 2.3 mL (22.25 mmols) of benzyl alcohol respectively. As for all the synthesis, the solutions were degassed under vacuum and heated form 200 °C to reflux temperature at a heating rate of 7 °C/minutes.

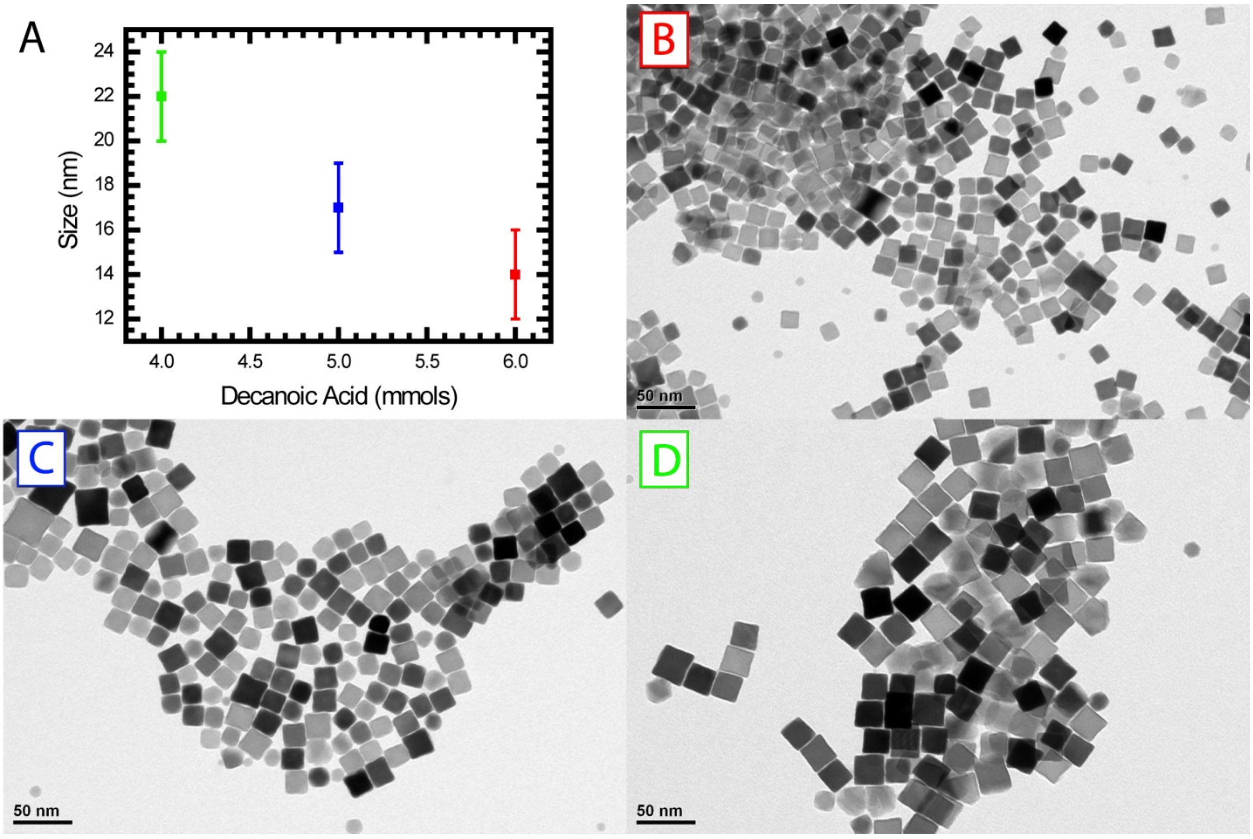

Figure S4. Size evolution as a function of the decanoic acid amount for iron oxide nanocubes synthesized using 15 mL of DBE, 10 mL of squalane, 7 °C/min heating ramp and 1 mmol of Iron(III) acetylacetoante (A). TEM images of iron oxide nanocubes of B) 14 ± 1.5 nm, C) 17 ± 2 nm and D 22 ± 3 nm synthesized using different molar amount of decanoic acid; B) 6 mmols C) 5 mmols and D) 4 mmols. Color labels (B, C and D) correspond to the plotted points in (A).

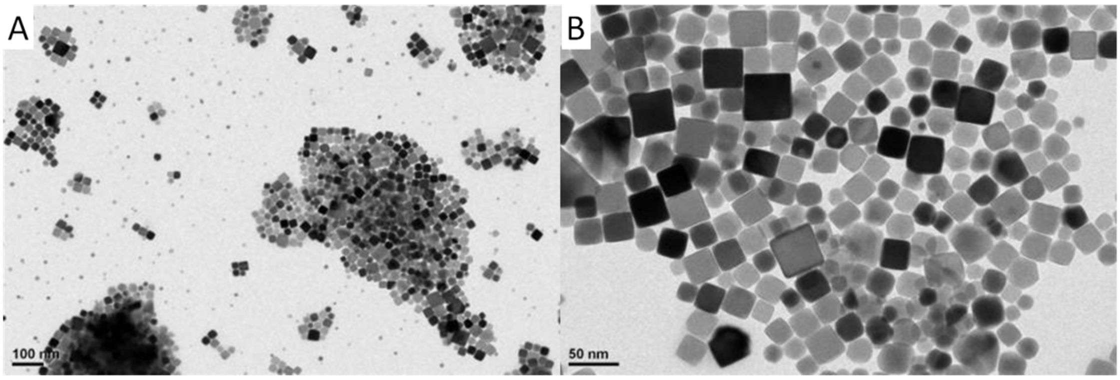

Figure S5. TEM images of 22 ± 4.5 nm iron oxide nanocubes synthesized by using 2 mmols of iron (III) acetylacetonate, 8 mmols of Decanoic acid, 18 mL of Dibenzyl ether and 32 mL of Squalane. The solution was degassed for 120 minutes at 65 °C before heating up to 200 °C (3 °C/min) under nitrogen atmosphere. After 2.5 hours the solution was heated up to reflux temperature (7 °C/min) and kept at this temperature for 60 minutes.

Synthesis of Gallic Acid PEG ligand

Synthesis of GA-PEG: To solution 7.5 g Poly(ethylene glycol) (PEG, 5 mmol, Mw=1500kDa) in 500 mL tetrahydrofuran (THF) stirred in round bottom flask, 850 mg of Gallic acid (GA, 5 mmol) dissolved in 200 mL THF and 60 mg dimethyl amino pyridine (DMAP, 0.5 mmol) dissolved in 20 mL THF is added and stirred at room temperature. The flask is equipped with a dropping funnel containing 5.2 g N.N'-Dicyclohexylcarbodiimide (DCC, 25 mmol) dissolved in 50 mL THF which is added drop-wise within 1h to the solution of PEG/GA/DMAP. The mixture is stirred at room temperature for 16 hours and THF and DMAP are removed under reduced pressure. The crude product GA-PEG is dissolved in 200 mL de-ionized water and the pH is adjusted to 2 to precipitated hydrolyzed DCC. After 1h, the solution is filtered with a paper filter and GA-PEG is extracted from the aqueous phase 3 times with 200 mL chloroform. After removal of Chloroform GA-PEG was dried in high vacuum for 5 hours prior to determination of the yield which is around 70%. A 0.1M solution of GA-PEG in chloroform was prepared and used for the injection to the IONPs synthesis solution.

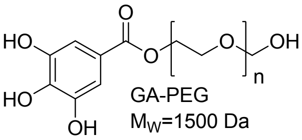

1H NMR (400 MHz, CDCl3): δ(ppm)= 6.98 (Ar-H), 4.64 (CH2-ester), 3.62-3.28 (CH2, OH-PEG)

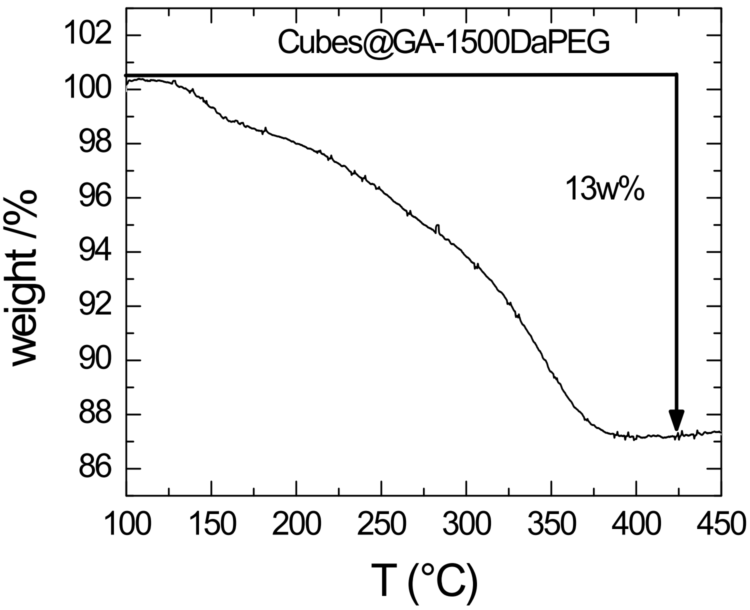

Figure S6. TGA analysis of a dried sample of 22 ± 2 nm iron oxide nanocubes bearing GA-PEG ligands. The sample was heated up under nitrogen atmosphere at 10°C/min and the weight loss, which corresponds to the organic component of the material, as a function of temperature, was recorded. 13% of the total mass weight was attributed to GA-PEG ligands while the amount of nanocubes corresponds to 87% of the total mass weight as found. Based on the unit cell and the nanocube size we calculate the molecular weight of each nanocube (3.323*107 g/mol) and knowing the molecular weight of GA-PEG (1653 g/mol) by using the following equation we can estimate the average number of GA-PEG molecules grafted per nanocube, which corresponds roughly to 3000 GA-PEG molecules :

$$\frac{N_{GA-PEG\,molecules}}{N_{cube}} = \frac{13\%}{1653 g/mol}\frac{3.323\ 10^{7} g/mol}{87\%} = 3004\ molecules/nancube$$

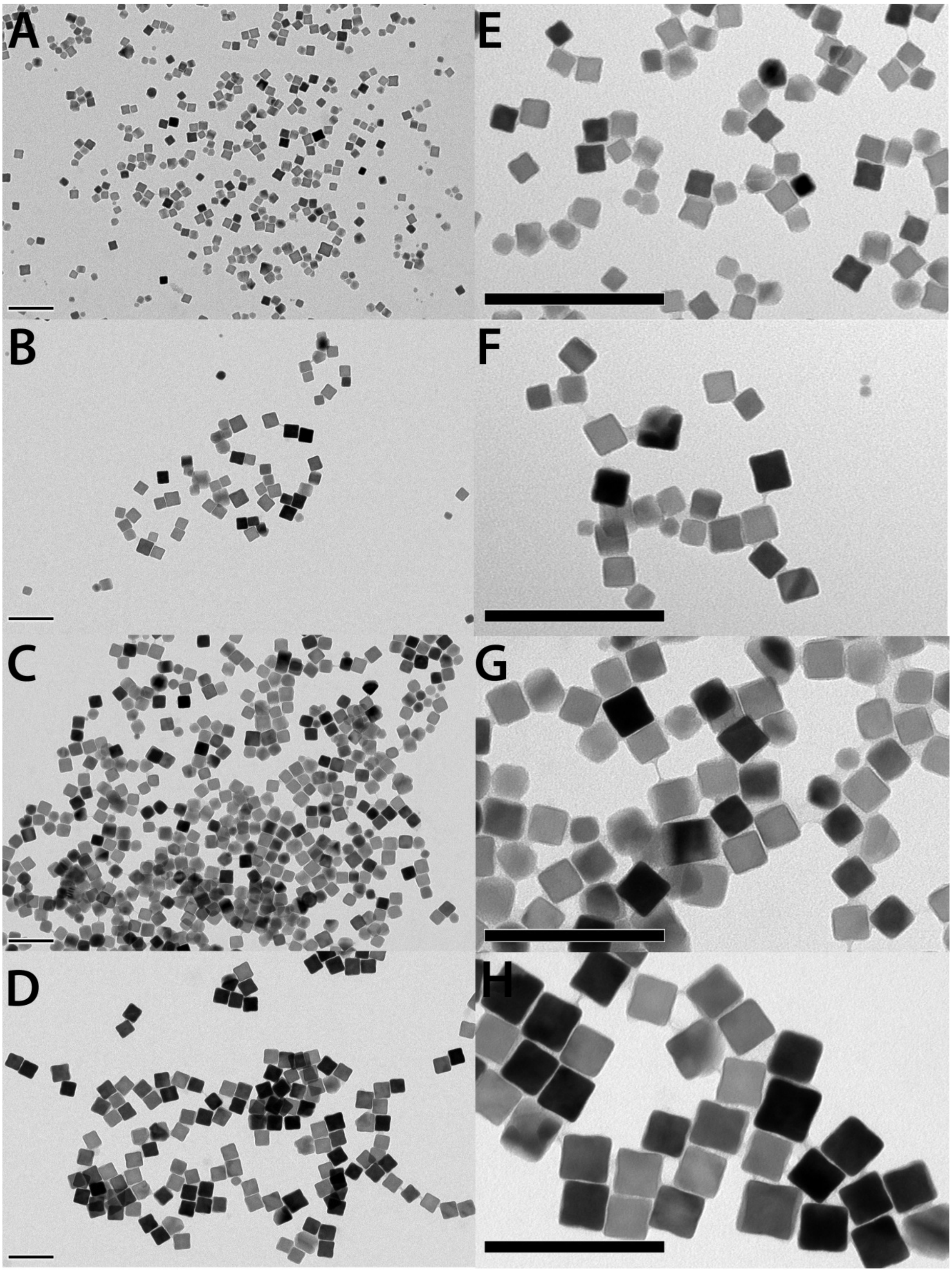

Figure S7. Transmission electron microscopy of water soluble iron oxide nanocubes synthesized of A, E) 14 ± 1.5 nm ; B, F) 19 ± 2 nm, C, G) 24 ± 2 nm and D, H) 35 ± 2nm synthesized using different synthesis conditions listed in Table S1. Scale bars correspond to 100 nm.

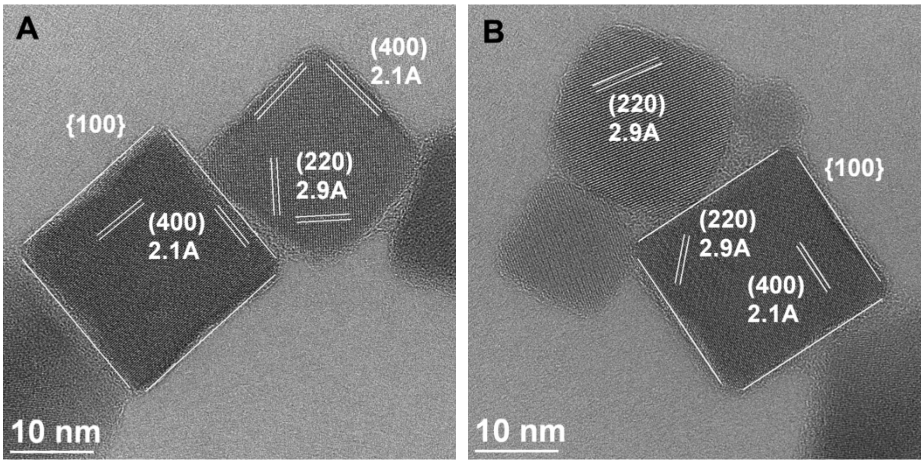

Figure S8. HRTEM images of IONCs, a) and b), exhibiting their typical cubic habit, defined by six {100} peripheral facets, and showing the typical spinel ferrite (220) and (400) lattice sets with d-spacing of 2.9 Å and 2.1Å, respectively (reference pdf card numbers 01-087-0244 86-1334). The NCs on the pictures are observed along the [001] zone axis.

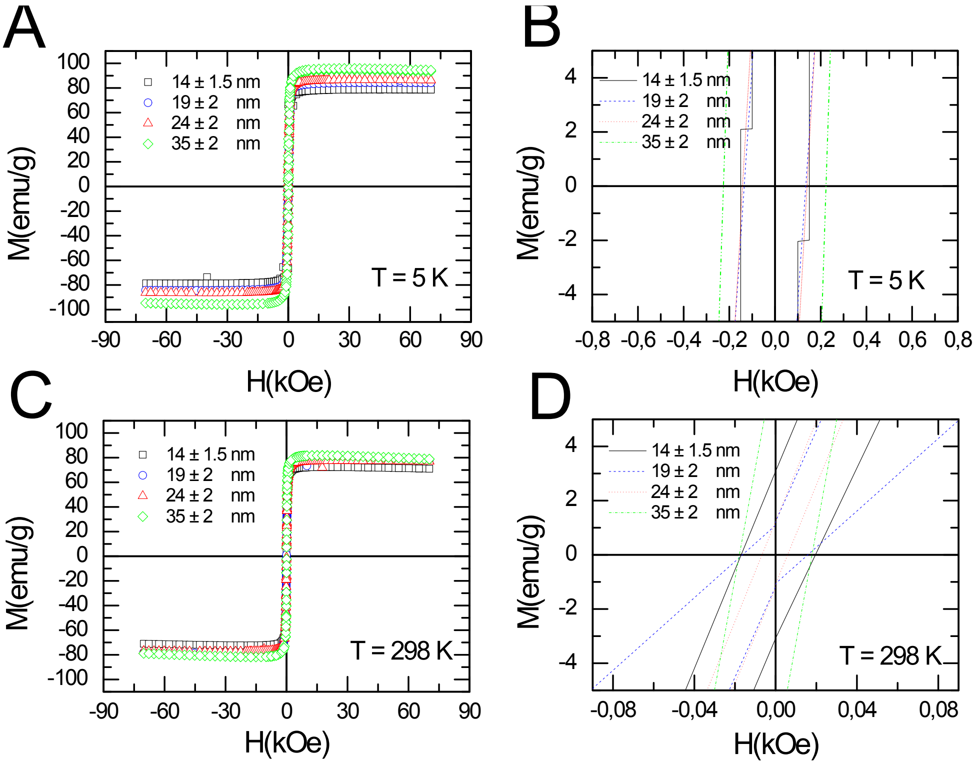

Figure S9. Hysteresis loops at 5 K (A) and 298 K (C) for 14 ± 1.5 nm (black square ☐), 19 ± 2 nm (blue circles ○), 24 ± 2 nm (red triangles ❐) and 35 ± 2nm (green rhombi ❋). Low field detail of the magnetization hysteresis loops (B and D), showing the coercive fields at 5 K (B) and 300 K (D) for 14 ± 1.5 nm (black line), 19 ± 2 nm (blue dash), 24 ± 2 nm (red dot line) and 35 ± 2nm (green dash-dot line).

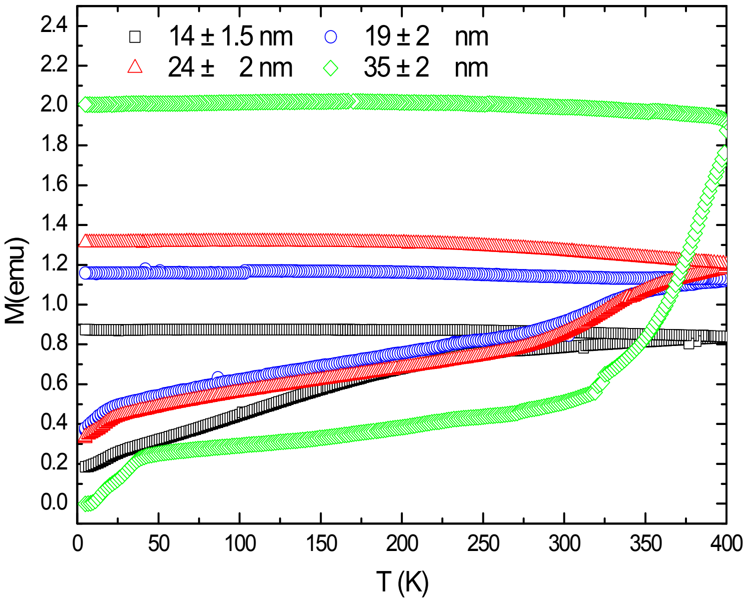

Figure S10. Temperature dependence of the zero field cooling and field cooling (cooling field H_{FC} = 25 Oe) magnetization curves measured at 25 Oe, as a function of particle size. Notice the higher blocking temperature (T_B) of the 35 ± 2 nm IONPs with respect the smaller samples.

Sample	M_S(5 K) emu/g	M_S(298 K) emu/g	H_C(5K) Oe	H_C(298K) Oe
35 ± 2	98 ± 10	88 ± 8	226 ± 5	23 ±3
24 ± 2	85 ± 8	75 ± 7	141 ± 4	7 ± 1
19 ± 2	82 ±8	73 ± 7	136 ± 4	28 ± 2
14 ± 1.5	74 ± 7	64 ± 6	152 ± 5	26 ± 2

Table S2. Summary of the magnetic data for 14 ± 1.5 nm, 19 ± 2 nm, 24 ± 2 nm and 35 ± 2nm water soluble iron oxide nanocubes. Due to the experimental error associated to the normalization of the saturation magnetization the values can show deviation of about a 10 %

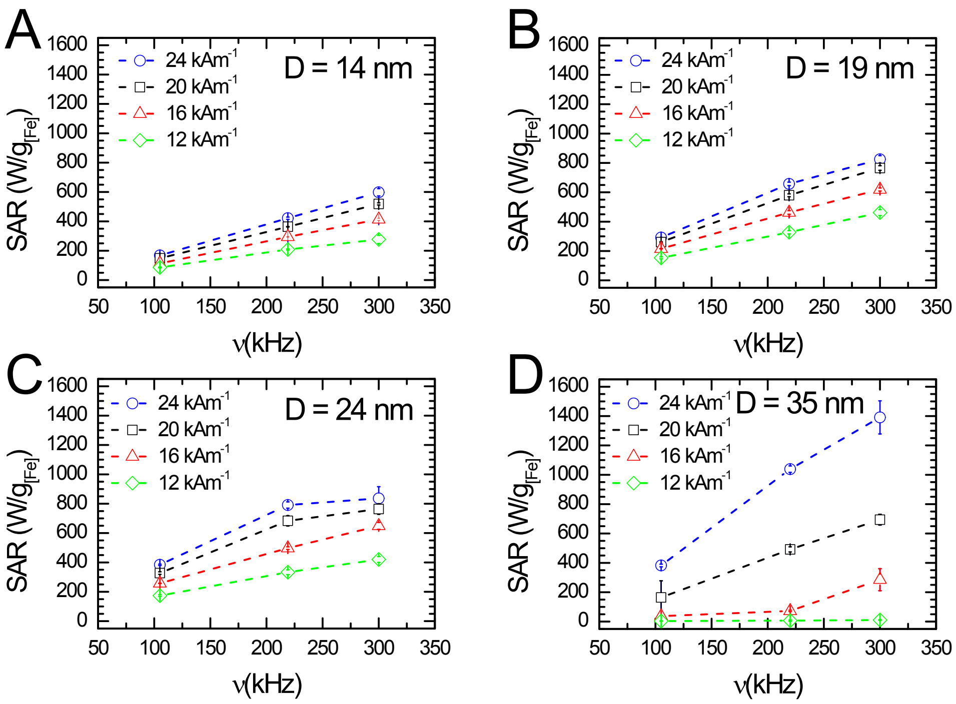

Figure S11. SAR values as a function of the frequency at different field amplitudes of 24 kAm^{-1} (blue circles ●,○), 20 kAm^{-1} (black squares ■,□). 16 kAm^{-1} (red triangles ▲, Δ) and 12 kAm^{-1} (green rhombi ✸,◊) for A) 14 ± 1.5 nm, B) 19 ± 2 nm, C) 24 ± 2 nm and D) 35 ± 2 nm. Each experimental data point was calculated as the mean value of at least 4 measurements and error bars indicate the standard deviation.

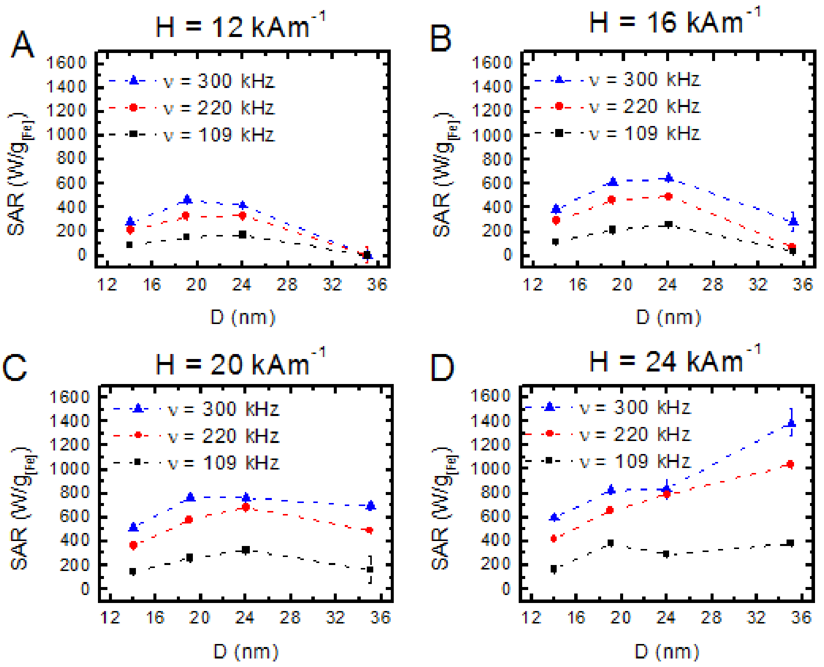

Figure S12. SAR values as a function of the size at different magnetic field amplitude of A) 12 kAm-1, B) 16 kAm^{-1}, C) 20 kAm-1 and D) 16 kAm^{-1} and at three different frequencies 300 kHz (blue triangles ▲), 220 kHz (red circles ●), and 109 kHz (black squares ■). Each experimental data point was calculated as the mean value of at least 4 measurements and error bars indicate the standard deviation.

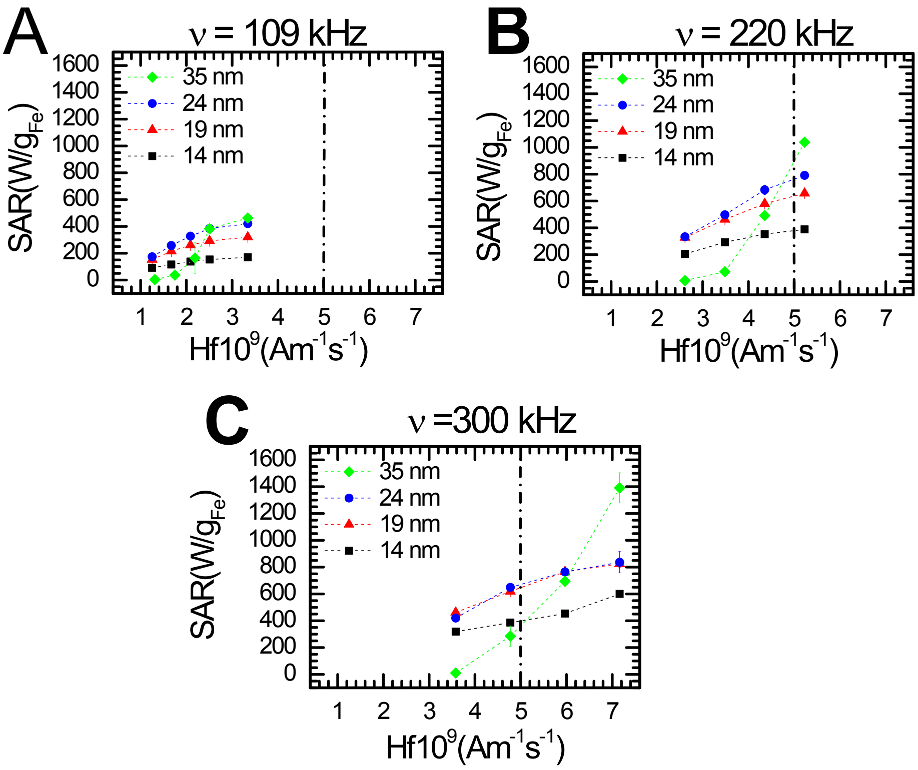

Figure S13. SAR values as a function of the Hf factor at A) 109 kHz, B) 220 kHz and C) 300 kHz for iron oxide nanocubes of 14 ± 1.5 nm (black squares ■), 19 ± 2 nm (red triangles ▲), 24 ± 2 nm (blue circles ●) and 35 ± 2 nm (green rhombi ✹). Each experimental data point was calculated as the mean value of at least 4 measurements and error bars indicate the mean deviation. Vertical dashed line corresponds to the biological limit ($Hf = 5\cdot10^{9}\,\mathrm{Am^{-1}s^{-1}}$).

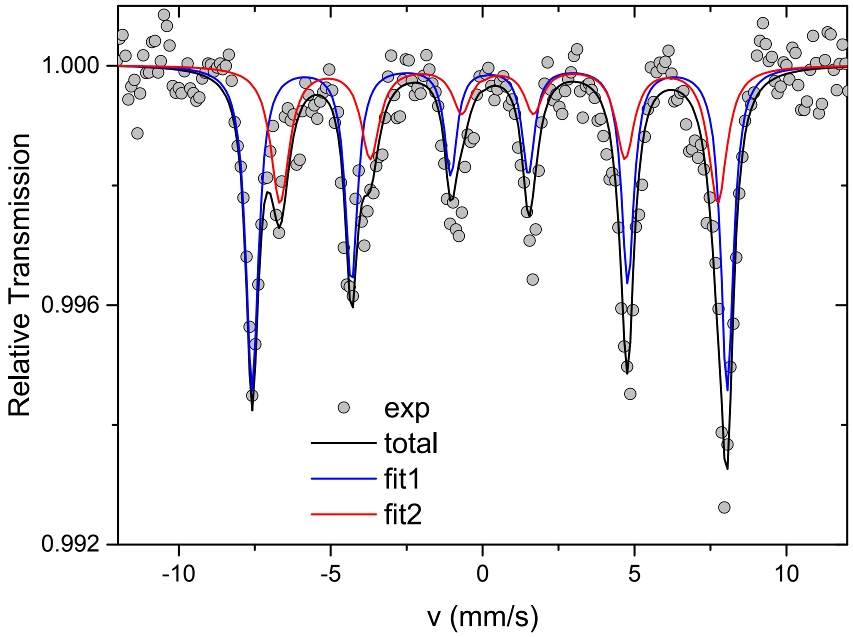

Figure S14. ^{57}Fe Mössbauer spectrum of water soluble nanocubes of 19 nm recorded at room temperature. As shown, the spectrum consists of sextet characteristic of magnetic ordering. The refinement has been performed with two magnetic components attributed to tetrahedral and octahedral Fe sites (Table R1) and neither hematite nor other iron oxidation degrees are detected. Values of the refined hyperfine parameters are consistent with those of the literature. Indeed value of isomer shift in the Td site (IS = 0.34(1) mm/s) indicates an high spin state of Fe3+ whereas the value in the Oh site (IS = 0.63(2) mm/s) is intermediate between high state of Fe2+ and Fe3+. Magnetite is an inverse spinel and above Verwey transition, there is an hopping mechanism between Fe2+ and Fe3+ which leads to this intermediate value of IS .

	δ (mm/s)	2ε (mm/s)	B_{hyp} (T)
T_d site	0.34(1)	0.00(1)	48.2(1)
O_h site	0.63(2)	0.04(4)	44.6(1)

Table S3: Mössbauer hyperfine parameters extracted from refinements of the 300K spectrum. δ is the isomer shift, 2ε is the quadripolar contribution and B_{hyp} is the hyperfine field.

Zero-field ^{57}Fe Mössbauer measurements were carried out at 300K in a transmission mode with constant acceleration using a ^{57}Co/Rh γ-ray source. The spectrometer was previously calibrated using a standard α-Fe foil and the isomer shift values were expressed with respect to this standard. The fitting of the spectrum was performed using the MOSFIT [*J.Teillet, F.Varret, unpublished MOSFIT Program (Universite du Maine, Le Mans, France)*] program with magnetic components composed of lorentzian lines.

TEM size (nm)	**Size by Number (nm)**	**Size by Intensity (nm)**	**Size by Volume (nm)**	**PdI**
35 ± 2 nm	37 ± 14	226 ± 120	48 ± 21	0.29
24 ± 2 nm	32 ± 12	133 ± 85	57 ± 44	0.27
19 ± 2 nm	31 ± 10	81 ± 41	45 ± 23	0.22
14 ± 2 nm	31 ± 9	59 ± 22	41 ± 16	0.12

Table S4. Summary of the DLS diameters in number% Intensity % and Volume % and of the PDI .